PSO/GA/ANN MODELING AND PREDICTION FOR THE HIGHER HEATING VALUES (HHVS) OF SOLID FUELS: THE MACHINE LEARNING APPROACH

Xiang Wang[1], Shanhui Zhao[1,*]

[1,*]Nanjing Institute of Technology, Nanjing 211167, China

[*]Corresponding author: shhzhaoseu@163.com

The quick evaluation for the higher heating value (HHV) is crucial for thermochemical conversion of solid fuels. In this work, machine learning method based on artificial neural networks (ANN) was used to predict the HHV of solid fuel. 205 groups of different kinds of solid fuels collected from publications were used. The proximate analysis, ultimate analysis and the combination of two were used as input parameters. The influence of activation function, neuron number and hidden layer number on the prediction performance was studied. Results show that single hidden layer with logsig function using 8 neurons was an optimized condition for HHV prediction. The combination of two composition analyses could achieve much higher accuracy, with the average relative error of 2.57%. Impact analysis indicated that the non-combustible components, namely ash content and oxygen content showed the largest influencing weight for HHV prediction, accounting for 21.73% and 22.91% respectively. Particle swarm optimization (PSO) and genetic algorithm (GA) were further used to optimize the artificial neural network model. Results show that PSO and GA both improved the prediction performance of ANN model by optimizing the initial weight and threshold values. The average relative errors for PSO-ANN and GA-ANN decreased to 1.15 % and 1.72 % respectively.

Key words*: Solid fuel; Higher heating value; Machine learning; Artificial neural network*

1. Introduction

Waste-to-Energy (WtE) represents a sustainable approach to managing solid waste by converting it into energy [1]. Thermochemical conversion technologies are important WtE technologies, which include incineration, pyrolysis and gasification, etc., in which solid fuels could be converted into heat, electricity, syngas, liquid fuels and chemicals. In the thermochemical conversion process, the characteristics of the fuel itself, including elemental composition, industrial analysis and its calorific value, are the key factors affecting the fuel conversion process and product distribution.

The heating value of solid fuels, also known as calorific value or energy content, is a crucial parameter that determines their suitability for various applications. The calorific value of solid fuel is usually measured experimentally by adiabatic bomb calorimeter [2]. However, the experimental measurement of fuel calorific value takes a lot of time, and in some cases, the data of fuel calorific value cannot be obtained quickly. Therefore, it is crucial to develop a fast method to estimate the calorific value of

solid fuels. In the past decades, some scholars have put forward a lot of empirical formulas for fuel calorific value prediction. In early period, the empirical formula was widely used to estimate the calorific value of coal or biomass. Dulong [3], Mason, García [4, 5] and other researchers proposed quite many empirical formulas, which were mainly based on the proximate analysis or ultimate analysis [6-8]. In recent years, with the development of solid waste treatment technologies, the evaluation methods for calorific values of solid waste is also put forward. Similarly, empirical formulas based on solid fuel composition are still the main methods. Bagheri et al. [9] introduced an empirical formula that contained the carbon and hydrogen content for evaluation of 252 MSW samples. Merza et al. [10] built an empirical formula that contains four element contents, namely C, H, N, S, O, to evaluate the HHV of 100 MSW samples. Similar works have also been done by Shi et al. [11], Kathiravale et al. [12] and other researchers.

The empirical formula is simple and fast, but its adaptability to raw materials is weak, and it can only predict some fuels with similar composition. Therefore, with the increasing types of solid fuels, the traditional empirical formula method has been unable to meet the increasing needs of fuel types and complexity.

In recent years, with the development of computer technology and artificial intelligence methods, the use of intelligent optimization algorithms or machine learning methods to build fuel calorific value prediction methods has become a more efficient and accurate means. For example, Tan et al. [13] used support vector regression for estimation of HHV of coal based on proximate analysis. The average absolute errors from estimating the HHV of Chinese and U.S. coals were only 2.16% and 2.42%. Lin et al. [14] used swift model for a lower heating value prediction for MSW. The model was applicable within this moisture range. Artificial Neural Networks (ANNs) represent the ultimate tool in modern computational modeling, where intricate patterns and correlations can be unraveled with unprecedented finesse. Taki et al. [15] used machine learning models for prediction the HHV of Municipal Solid Waste. The Artificial Neural Network (ANN) was used and proved that ANN's can be used as a practical tool with high accuracy and reliability for HHV evaluation. Güleç et al. [16] used ANN modeling for prediction of HHV of biomass. The proximate and ultimate analyses were taken as the basic data. The commonly used statistical values, namely correlation coefficient (R^2) and mean square error (MSE), were used to evaluate the modeling performance. Results show that ANN models trained by the combination of ultimate and proximate analyses datasets provided more accurate predictions than the models trained by individual ultimate analysis or proximate analysis datasets. However, only biomass materials were studied and industrial waste and coal were not taken into consideration.

Aiming at the urgent need of fast prediction method for high calorific value of different kinds of solid fuels, artificial neural network model is used in this paper to establish fast and accurate prediction model for biomass, domestic waste, industrial waste and coal. On this basis, the influences of input parameters and neural network structure parameters on prediction accuracy are analyzed. Particle swarm optimization (PSO) and genetic algorithm (GA) are further used to optimize the artificial neural network model, so as to further improve the prediction accuracy of the model. This work provides a more efficient theoretical method for the characteristic analysis of solid fuels and the application of thermochemical conversion technologies.

2. Classic empirical formula for estimating calorific value

In the past decades, there are quite some methods have been explored for quickly estimating the caloric values of solid fuels. In the early years, most empirical formulas were used to quickly predict the calorific value of fuels like coal [17]. Classical empirical models include those proposed by Dulong et al., Mason et al. and other researchers [7, 8]. These models are mainly based on ultimate analysis or proximate analysis results of coal.

Table 1. Classic empirical formula for estimating calorific value from publications

Publications	Correlation for HHV	Fuel types
Dulong et al. [17]	HHV=0.3383C+1.44(H-O/8)+0.0942S	Coal
Dulong et al. [3]	HHV=81C+342.5(H-O/8)+22.5-6(9H-W)	MSW/Coal
Boi et al. [12]	HHV=83.22C+274.3H-25.8O+15N+9.4Cl+65P	Refuse
Bento et al. [3]	HHV=44.75VM-5.85W+21.2	Refuse
Mott et al. [12]	HHV=0.336C+1.418H-0.0145O+0.0941S	Coal/Refuse
Neavel et al.	HHV=145.9C+569.6H-53.89O+43.08S-6.3Ash	Coal

As shown in **Tab.1**, most empirical formulas that proposed by different researches are mainly based on the elemental composition. These empirical formulas could give an estimation for specific fuel. Because of the fitting of empirical formulas, mainly for specific fuels, these empirical formulas cannot be adapted to many different fuels. For example, coal, biomass, domestic waste, etc., these fuels have significant differences in composition, so the traditional empirical formulas cannot meet the estimation of the calorific value of different types of fuels. With the increasing combustion disposal of solid waste in recent years, there is a need for more general methods for estimating the calorific value of different fuels, especially for combustible solid waste.

3. The ANN modeling method

3.1. The composition of solid fuels

With respect to solid fuels, there are mainly two analysis methods, namely proximate analysis and ultimate analysis. Proximate analysis provides information about the major components of a material, typically focusing on moisture content (MC), volatile matter (VM), fixed carbon (FC), and ash content (A). It gives a snapshot of the solid fuel's composition and properties that are important for its handling and utilization. Ultimate analysis gives a more detailed breakdown of the elemental composition of a material, usually determining the percentages of C, H, N, S, and O (if applicable). It provides deeper insight into the chemical structure and potential energy content of the solid fuel.

For the calorific value of fuel, ultimate analysis and proximate analysis have a key impact. Therefore, the composition and HHVs of different types of solid fuels were collected from publications[18-23] and are listed in **appendix file**.

A total of 205 groups of solid fuel samples were collected from publications. Because the moisture of the fuel has a significant effect on the composition ratio and the calorific value of the fuel, the dry basis of the fuel is used in this paper to eliminate the influence of external moisture fluctuations. The proximate analysis (ash content, volatile matter and fixed carbon) and ultimate analysis (C, H, N, S, O) were used as the main composition. With respect to biomass waste, there are other component analysis methods, such as cellulose, hemicellulose and lignin, were not taken into consideration in this work.

By analyzing the composition of different solid fuels, it can be seen that the ash content varies from 0.02% (PP) to 39.82% (fish bond). In general, the ash content of woody biomass and plastics is generally low, while the ash content of rice husk, rice straw, rubber and food residue is high. The volatile matter contents of biomass and plastics are much higher than fixed carbon contents. The highest volatile content is 99.97% for PP, which means that almost all combustible matters are released during pyrolysis as volatiles. The wooden biomass samples have relative higher fixed carbon content.

The HHV results for these solid fuels vary from 13.29 MJ/kg (Vine shoot waste) to 46.47 MJ/kg (PE). Generally speaking, fuels with high ash content and high oxygen content tend to have lower calorific values, whereas fuels with low ash content and high carbon content, such as plastics, have higher calorific values.

3.2. The building of the ANN model

In this section, machine learning algorithms will be used to construct prediction models for high calorific value of complex fuels. BP artificial neural network, or Backpropagation artificial neural network (BP-ANN), is a type of neural network widely used in machine learning and artificial intelligence.

As discussed above, the HHV of solid fuel mainly depends on the elemental composition and proximate analysis of the raw material. With respect to the input layer of the BP-ANN model, there are three kinds of networks are built in this work as follows.

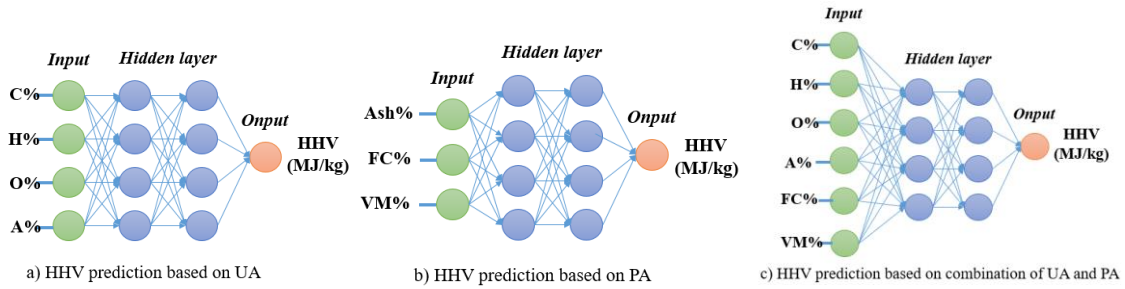

a) HHV prediction based on UA b) HHV prediction based on PA c) HHV prediction based on combination of UA and PA

Figure 1. The configurations of three networks based on different input parameters

As shown in **Fig.1**, different input parameters are chosen to predict the HHV of solid fuels. **Fig.1(a)** shows that the ultimate analysis, namely C, H, O, A (ash) are used as the input parameters, as model-1. Proximate analysis, namely Ash, FC (fixed carbon) and VM (volatile matter) are used in model-2, as shown in **Fig.1(b).** Model-3 combines ultimate analysis and proximate analysis, as shown in **Fig.1(c)**.

The determination of the optimal number of neurons in the hidden layer significantly impacted the predictive accuracy of the network [24]. Consequently, the influence of neuron quantity on prediction performance was carefully evaluated. According to the theory of Artificial Neural Networks [25], the appropriate number of neurons could be determined using the following empirical formula [26]:

$$\mathrm{h} = \sqrt{m+n} + a \tag{1}$$

In this formula, h represents the number of neurons in the hidden layer, m denotes the number of nodes in the input layer, and n indicates the number of neurons in the output layer. The parameter a is an adjustment constant ranging from 1 to 10. To achieve optimal prediction accuracy and prevent overfitting, the optimal number of neurons was determined through trial and error [27], with h varying between 3 and 12.

In neural networks, the hidden layer's activation function, often referred to as the "transfer function," plays a crucial role in determining the output of each neuron in that layer. Common activation functions are summarized as follows:

$$\text{Sigmoid Function: } f(x) = \frac{1}{1+e^{-x}} \quad (2)$$

$$\text{Hyperbolic Tangent (tanh): } f(x) = \frac{1-e^{-x}}{1+e^{-x}} \quad (3)$$

$$\text{purlin function: } f(x) = x \quad (4)$$

Sigmoid function (*Logsig*) is a Smooth, S-shaped curve. It maps input values to a range between 0 and 1, which is useful for probabilities. Hyperbolic Tangent function (*tansig*) is also smooth and S-shaped but maps input values to a range between -1 and 1. It often performs better than the sigmoid function due to its zero-centered output. In this work, the *logsig* and *tansig* functions were chosen as the activation function for hidden layer. The prediction performance was compared.

The performance of the ANN models was evaluated using the mean square error (MSE), which is defined as follows:

$$\text{MSE} = \frac{1}{N}\sum_{i=1}^{N}(Y_{Model} - Y_{Exp})^2 \quad (6)$$

In which, the Y_{Model} is the output results by the ANN model, Y_{Exp} is the experimental data, and the N is the number of the samples.

A total of 205 sets of data were used for the construction and verification of ANN model, among which 197 sets of data were used for the training, validation and testing of the model. To enhance the predictive capability of the ANN model, the datasets were partitioned randomly into training (70%), validation (15%), and test (15%) subsets, which are adopted by other works [28, 29]. The network underwent training utilizing the Levenberg-Marquardt backpropagation algorithm, with a learning rate of 0.01 and a training target minimum error of 0.0001. Eight sets of data (Fruit peel, Wood, Newspaper, PE, Rubber, Coconut shell, Vegetal coal and Rice straw) were used for checking the performance of the model.

All the calculation was conducted on the commercial software of Matlab® R2020b (Mathworks, Inc., Natick, MA, USA).

4. Results and discussion

4.1. ANN modeling results

Firstly, the effect of the hidden layer on the ANN modeling performance was studied. Three kinds of hidden layer activation function, namely single layer with *Logsig* function, single layer with *Tansig* function, two layer with *Tansig-Logsig* function were compared. The effect of the neuron number was compared for each kind of hidden layer. The results are summarized in **Fig.2** as follows.

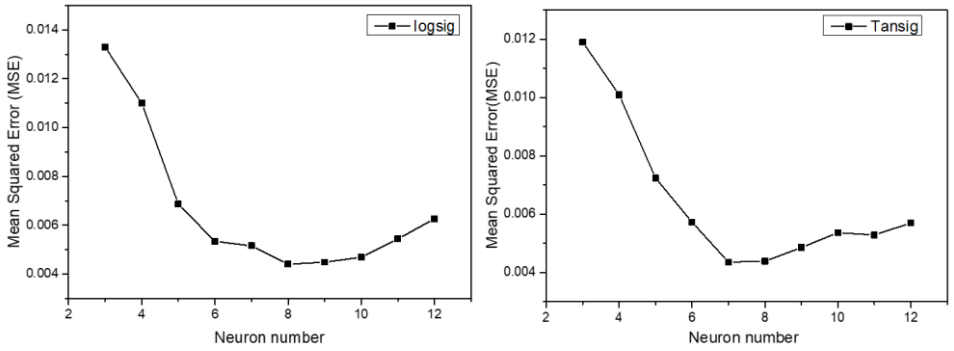

(a)Single hidden layer: Logsig (b) Single hidden layer: Tansig

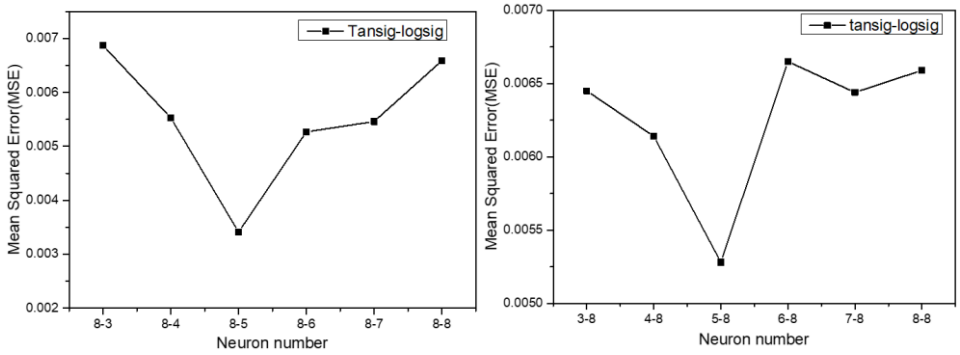

(c)Two hidden layer: Tansig-Logsig (d) Two hidden layer: Tansig-Logsig

Figure 2. The effect of hidden layer on the ANN performance

As shown in **Fig.2**, both the activation function, hidden layer number and neuron number have effect on the modeling performance. As for single hidden layer in **Fig.2(a)** and **Fig.2(b)**, the MSE value initially decreased with neuron number and reached a minimum of 0.00441 and 0.00436 at neuron number of 8 and 7 for Logsig and Tansig function respectively. Further adding neuron number, the prediction performance decreased. This phenomenon is due to overfitting caused by an excessive increase in the number of neurons [30]. Similar tendency occurs for two hidden layer cases in **Fig.2(c)** and **Fig.2(d)**. The two-layer case reached minimum of 0.00341 at 8-5 (8 neurons for Tansig and 5 neurons for Logsig layer). Therefore, there is an optimized neuron number for all the cases.

Although the two-layer hidden network has the lowest MSE value, it is also more prone to overfitting. Therefore, overall, using a single hidden layer neural network with Logsig can balance prediction effectiveness and better avoid overfitting. Consequently, in the subsequent models presented in this paper, a single Logsig hidden layer is adopted as the basic structure of the neural network for modeling and predicting the calorific value of different fuels.

Next, the detailed prediction performance for three models, namely ANN-1, ANN-2 and ANN3 are compared with experiment data. Eight groups of solid fuels are used. The results are shown in **Fig.3** as follows.

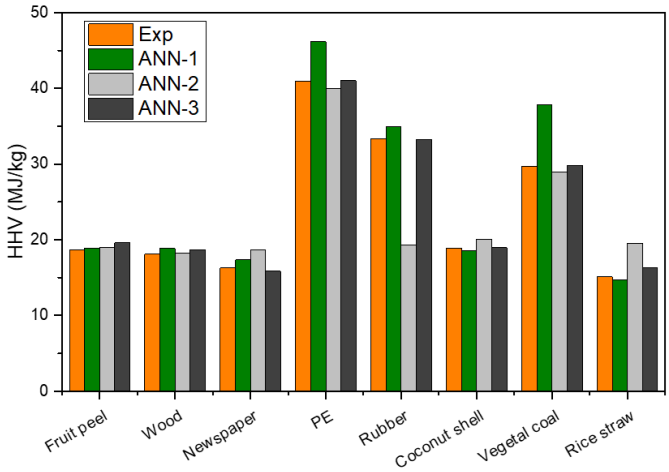

Figure 3. The comparison prediction performance of different ANN models

As shown in **Fig.3**, ANN-1, ANN-2 and ANN-3 refer to three models that have been discussed in **Fig.1** above. ANN-1 uses ultimate analysis as input parameter, that show quite good performance for fruit peel, wood, newspaper, rubber, coconut shell and rice straw. However, three is some difference for PE and vegetal coal. ANN-2 uses proximate analysis, which shows good performance for most samples except for rubber. ANN-3 combines ultimate analysis and proximate analysis as input parameters, that show the best performance among three models.

In order to further analyze the prediction performance among three models, the relative prediction errors (RPE) were calculated according to the formula as follows:

$$\mathrm{RPE} = \frac{abs(Y_{exp} - Y_{model})}{Y_{exp}} \times 100\% \quad (7)$$

Based on formula (7), the RPE of three models are calculated and the results are summarized in **Tab.2** as follows.

Table 2. The relative prediction errors for three models

Sample	Relative prediction error(%)		
	ANN-1	ANN-2	ANN-3
Fruit peel	1.40	2.08	5.26
Wood	4.03	0.77	3.31
Newspaper	6.58	15.12	2.58
PE	12.71	2.34	0.12
Rubber	4.58	42.07	0.39
Coconut shell	1.48	6.30	0.37
Vegetal coal	27.40	2.63	0.34
Rice straw	2.65	29.56	8.22
Average	7.60	12.61	2.57

As shown in **Tab.2**, the largest RPE value for ANN-1 are 27.4% (Vegetal coal). The largest RPEs for ANN-2 are 42.07% (Rubber). It seems that individual ultimate analysis or proximate analysis can hardly to cover all samples to obtain high prediction accuracy. With respect to ANN-3, the largest RPE is as low as 8.22% (rice straw), which is much lower than ANN-1 and ANN-2. Based on individual RPE, the average RPEs for three models are 7.60%, 12.61% and 2.57%. It's significant that ANN-3 has the best prediction performance, while ANN-2 shows the worst performance. Besides, the largest RPE is no more than 10% for ANN-3, which proves that ANN-3 is an effective method for HHV prediction of solid fuels.

4.2. The network weight analysis

The weight and bias of the network is a crucial parameter for the ANN modeling. In order to reveal the relative influent of each input parameter on the ANN modeling prediction performance, the weight and bias values of the ANN-3 were calculated and analyzed. The weight values that are corresponding to each input parameter and the bias values are summarized in **Tab.3** as follows.

Table 3. The weight and bias values of the hidden layers in ANN-3 model

	Input parameters						
Neuron	W_{Ash}	W_{VM}	W_{FC}	W_C	W_H	W_O	Bias
1	1.8717	0.0923	0.0774	-2.0777	0.3542	-2.8471	-4.0945
2	2.4723	-1.1051	2.1537	0.3186	-0.1165	-1.9461	-2.8110
3	-1.6171	0.8509	2.4368	0.7953	1.843	-1.8731	2.1413
4	-2.0877	-2.5879	0.8235	1.7737	-1.2135	0.1477	-0.7313
5	1.5048	-1.5501	2.1769	3.317	0.295	-0.275	0.4881
6	0.8305	-1.2765	2.0813	2.7808	2.1748	0.0957	-1.3645
7	-1.6733	0.7295	0.9754	-0.9593	1.1753	-2.2153	-2.8354
8	1.6079	-2.0673	-0.023	0.3029	2.5834	1.5864	3.9613

As shown in T**ab.3**, the 7×8 matrix represents the weight values between the input layer and the hidden layer nodes. W_{Ash}, W_{VM}, W_{FC}, W_C, W_H and W_O represent the weight of proximate analysis and ultimate analysis parameters respectively.

Based on the weights values in **Tab.3**, the relative influence of the input variables on the ANN model outputs were calculated by formula (8) as follows[31-33]:

$$I_i = \frac{\sum_{j=1}^{j=n}\left[\left(\frac{|IW_{j,i}|}{\sum_{i=1}^{i=m}|IW_{j,i}|}\right)\cdot|LW_{k,j}|\right]}{\sum_{i=1}^{i=m}\left\{\sum_{j=1}^{j=n}\left[\left(\frac{|IW_{j,i}|}{\sum_{i=1}^{i=m}|IW_{j,i}|}\right)\cdot|LW_{k,j}|\right]\right\}} \quad (8)$$

In this context, *i* and *m* denote the *i*th neurons in the input layer and their respective indices. Similarly, *j* and n refer to the *j*th neurons in the hidden layer and their indices. *k* represents the *k*th neuron in the output layer. I_i signifies the relative influence of the *i*th input variable on the kth output variable. $IW_{j,i}$ denotes the weight from the ith input variable to the *j*th neuron in the hidden layer. $LW_{k,j}$ represents the weight from the *j*th neuron in the hidden layer to the kth neuron in the output layer. By calculating the I_i, the relative impact of *i*th input variable on the *k*th output could be obtained. The relative influence of six input variables on the HHV prediction performance are calculated and the results are shown in **Fig.4** as follows.

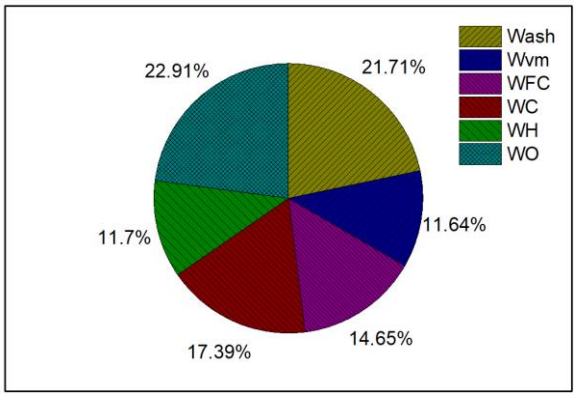

Figure 4. The relative impact analysis of input variables on ANN prediction performance

As show in **Fig.4**, among six parameters in input layer, the ash content and oxygen content contribute the leading impact on the HHV prediction, which are 21.71% and 22.91% respectively. As known that oxygen and ash are non-combustible composition for solid fuels, which will lower the HHV of solid fuels. With respect to combustible component, carbon content shows the highest impact on HHV prediction, which is about 17.39%. Volatile matter shows the lowest impact. The reason is that the composition of volatile matter is complicated, which contains not only combustible components, such as CO, H_2, CH_4, but also non-combustible species, such as CO_2, H_2O. Therefore, the impact of volatile matter is weakened. The impact of hydrogen content is also quite low, which is attributed to the low concentration in solid fuels (no more than 10 wt%, as shown in **Tab.2**). Therefore, hydrogen contributes less to the HHV than carbon element.

4.3. The ANN optimization by PSO and GA algorithms

In this work, two advanced optimization algorithms, namely the genetic algorithm (GA) and particle swarm optimization (PSO), were employed to optimize the initial weights and threshold values of the network. PSO, pioneered by Kennedy and Eberhart [34, 35], is renowned for effectively addressing multidimensional nonlinear problems. Moreover, ANN predictions are prone to local optima and overfitting [36], as pointed out above. One notable advantage of the PSO-ANN approach is its capability to mitigate the risk of falling into local optima [26, 36, 37]. Therefore, integrating the PSO algorithm with the ANN model enhances prediction accuracy and accelerates convergence during both network training and prediction phases.

Similarly, genetic algorithms (GA) represent another optimization method that emulates natural heredity and biological evolution, which is used to optimize the weight and threshold values of ANN models. The genetic algorithm identifies the individual with the optimal fitness value through selection, crossover, and mutation operations. Subsequently, the GA initializes the optimized weight and threshold values derived from the optimal individual for the network, enhancing the network's prediction performance.

The principle and flowsheet of ANN model optimized by PSO and GA algorithms was summarized in **Fig. 5** as follows.

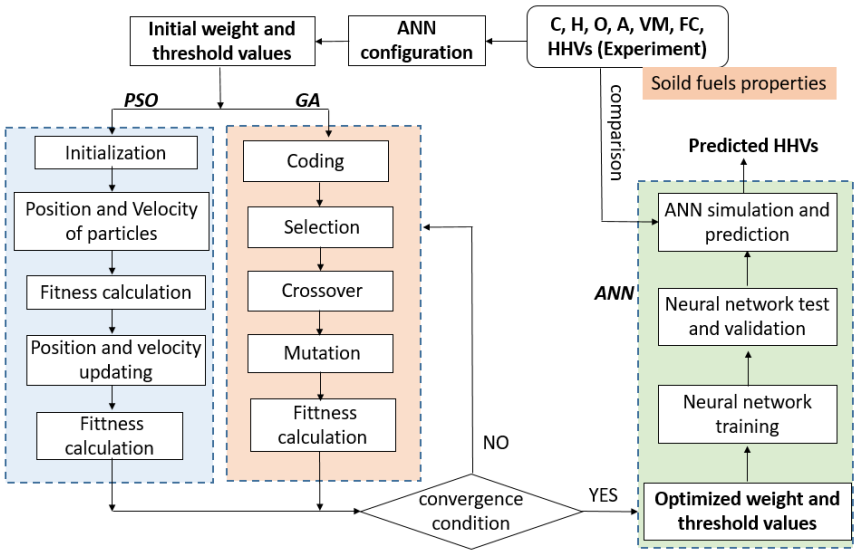

Figure 5. The flowsheet of the ANN model optimized by PSO and GA algorithms

As shown in **Fig.5**, instead of random generation of the initial weight and threshold values of the ANN, the initial weight and threshold values are optimized by GA and PSO respectively. The optimized weights and threshold values are then assigned to the ANN model.

The comparison of experiment results with prediction results of ANN, PSO-ANN and GA-ANN models was conducted and summarized in **Fig.6** as follows.

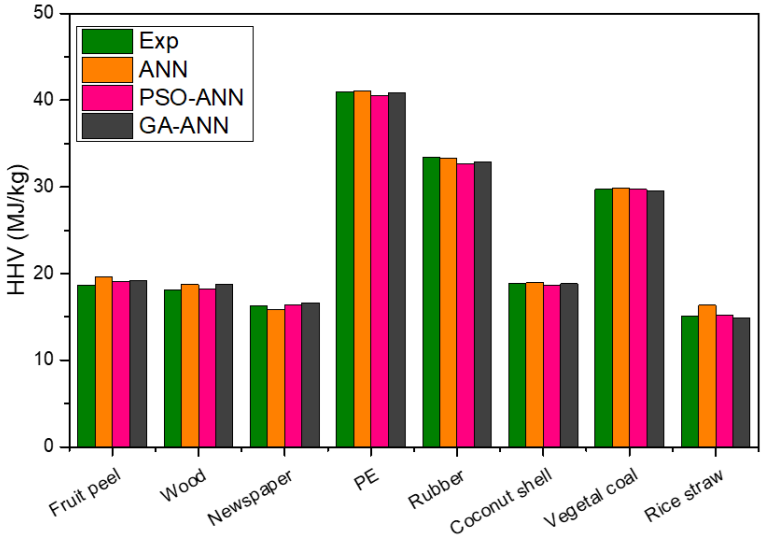

Figure 6. The comparison prediction performance of ANN, PSO-ANN and GA-ANN models

From **Fig.6**, it can be seen that GA and PSO can improve the prediction accuracy of ANN model, e.g. for fruit peel, newspaper, while there is a decreases for rubber. In order to analyze the prediction accuracy of the three models more clearly, the relative errors are calculated and analyzed, and the results are shown in **Tab.4**.

Table 4. The relative prediction errors for three models

Samples	Relative prediction error(%)		
	A NN	PSO-ANN	GA-ANN
Fruit peel	5.26	2.15	3.22
Wood	3.31	0.83	3.70
Newspaper	2.58	0.68	2.21
PE	0.12	1.20	0.44
Rubber	0.39	2.25	1.65
Coconut shell	0.37	1.01	0.37
Vegetal coal	0.34	0.07	0.64
Rice straw	8.22	1.06	1.52
Average	2.57	1.15	1.72
MSE	0.00441	0.00355	0.00382

It can be seen that the largest relative prediction error for three models are 5.26 % (ANN, fruit peel), 2.25 % (PSO-ANN, rubber) and 3.7 % (GA-ANN, wood). It's significant that PSO and GA algorithms could improve the ANN prediction accuracy and lower the error. Besides, the average errors of three models for eight samples are 2.57 %, 1.15 % and 1.72 % respectively. Similarly, the MSE of three models are 0.00441, 0.00355 and 0.00382 respectively, which also prove the optimization by PSO and GA algorithms. Although ANN-3 has been able to accurately predict the

high calorific value of different types of solid fuels, and PSO and GA can further improve its prediction accuracy, so the combination of this optimization algorithm and machine learning can be used to predict the high calorific value of fuel quickly and accurately. This method has a strong application prospect.

5. Conclusion

In this work, machine learning method based on artificial neural networks (ANN) was used to predict the HHV of solid fuel. The main conclusions are summarized as follows:

(1) Results show that single hidden layer with *logsig* function using 8 neurons was an optimized condition for HHV prediction. The total regression value is 0.95288.
(2) The combination of two composition analyses could achieve much higher accuracy, with the average relative error of 2.57%.
(3) Impact analysis indicated that the non-combustible components, namely ash content and oxygen content showed the largest influencing weight for HHV prediction, accounting for 21.73% and 22.91% respectively.
(4) Results show that PSO and GA both improved the prediction performance of ANN model by optimizing the initial weight and threshold values. The average relative errors for PSO-ANN and GA-ANN decreased to 1.15 % and 1.72 % respectively.

References

[1] Adeleke, O., et al., *Prediction of the heating value of municipal solid waste: a case study of the city of Johannesburg.* International Journal of Ambient Energy, 2022. **43**(1): p. 3845-3856.
[2] Dashti, A., et al., *Review of higher heating value of municipal solid waste based on analysis and smart modelling.* Renewable and Sustainable Energy Reviews, 2021. **151**: p. 111591.
[3] Liu, J.-I., R.D. Paode, and T.M. Holsen, *Modeling the energy content of municipal solid waste using multiple regression analysis.* Journal of the Air & Waste Management Association, 1996. **46**(7): p. 650-656.
[4] García, R., et al., *Spanish biofuels heating value estimation. Part I: Ultimate analysis data.* FUEL - GUILDFORD-, 2014. **117**(1).
[5] Pizarro, C., A. Lavín, and J.L. Bueno], *Spanish biofuels heating value estimation. Part II: Proximate analysis data.* Fuel, 2014.
[6] Mott, R.A. and C.E. Spooner, *The calorific value of carbon in coal: The Dulong relationship.*
[7] Mason, D.M. and K.N. Gandhi, *Formulas for calculating the calorific value of coal and coal chars: Development, tests, and uses.* Fuel Processing Technology, 1983. **7**(1): p. 11-22.
[8] Huang, Y.-F. and S.-L. Lo, *Predicting heating value of lignocellulosic biomass based on elemental analysis.* Energy, 2020. **191**: p. 116501.
[9] Bagheri, M., et al., *A comparative data mining approach for the prediction of energy recovery potential from various municipal solid waste.* Renewable and Sustainable Energy Reviews, 2019. **116**: p. 109423.
[10]Meraz, L., et al., *A thermochemical concept-based equation to estimate waste combustion enthalpy from elemental composition☆.* Fuel, 2003. **82**(12): p. 1499-1507.
[11] Shi, H., et al., *Characterization, thermochemical conversion studies, and heating value modeling of municipal solid waste.* Waste management, 2016. **48**: p. 34-47.
[12] Kathiravale, S., et al., *Modeling the heating value of Municipal Solid Waste☆.* Fuel, 2003. **82**(9): p. 1119-1125.
[13] Tan, P., et al., *Estimation of higher heating value of coal based on proximate analysis using support vector regression.* Fuel Processing Technology, 2015. **138**: p. 298-304.
[14] Lin, C.-J., et al., *Swift model for a lower heating value prediction based on wet-based physical components of municipal solid waste.* Waste management, 2013. **33**(2): p. 268-276.
[15] Taki, M. and A. Rohani, *Machine learning models for prediction the Higher Heating Value (HHV) of Municipal Solid Waste (MSW) for waste-to-energy evaluation.* Case Studies in Thermal Engineering, 2022. **31**: p. 101823.
[16] Güle, F., et al., *Predictability of higher heating value of biomass feedstocks via proximate and ultimate analyses – A comprehensive study of artificial neural network applications.* Fuel, 2022. **320**: p. 123944-.
[17] Mondal, C., et al., *Analysis and significance of prediction models for higher heating value of coal: an updated review.* Journal of Thermal Analysis and Calorimetry, 2023. **148**(15): p. 7521-7538.

[18] Zhou, H., et al., *Classification and comparison of municipal solid waste based on thermochemical characteristics.* Journal of the Air & Waste Management Association, 2014. **64**(5): p. 597-616.
[19] Güleç, F., et al., *Predictability of higher heating value of biomass feedstocks via proximate and ultimate analyses–A comprehensive study of artificial neural network applications.* Fuel, 2022. **320**: p. 123944.
[20] Yin, C.-Y., *Prediction of higher heating values of biomass from proximate and ultimate analyses.* Fuel, 2011. **90**(3): p. 1128-1132.
[21] Zhao, L., et al., *Characterization of Singapore RDF resources and analysis of their heating value.* Sustainable Environment Research, 2016. **26**(1): p. 51-54.
[22] Nhuchhen, D.R. and P.A. Salam, *Estimation of higher heating value of biomass from proximate analysis: A new approach.* Fuel, 2012. **99**: p. 55-63.
[23] Sheng, C. and J. Azevedo, *Estimating the higher heating value of biomass fuels from basic analysis data.* Biomass and bioenergy, 2005. **28**(5): p. 499-507.
[24] Jiao, B. and Y.E. Mingxing, *Determination of Hidden Unit Number in a BP Neural Network.* Journal of Shanghai Dianji University, 2013.
[25] Serrano, D., I. Golpour, and S. Sánchez-Delgado, *Predicting the effect of bed materials in bubbling fluidized bed gasification using artificial neural networks (ANNs) modeling approach.* Fuel, 2020. **266**: p. 117021.
[26] Zhao, S., W. Xu, and L. Chen, *The modeling and products prediction for biomass oxidative pyrolysis based on PSO-ANN method: An artificial intelligence algorithm approach.* Fuel, 2022. **312**: p. 122966.
[27] Estiati, I., et al., *Fitting performance of artificial neural networks and empirical correlations to estimate higher heating values of biomass.* Fuel, 2016. **180**: p. 377-383.
[28] Kuppusamy Y, Jayaseelan R, Pandulu G, et al. *Artificial neural network with a cross-validation technique to predict the material design of eco-friendly engineered geopolymer composites*. Materials, 2022, **15**(10): p. 3443.
[29] Ramachandra S, Durodola J F, Fellows N A, et al. *Experimental validation of an ANN model for random loading fatigue analysis*. International Journal of Fatigue, 2019, **126**: p.112-121.
[30] Tetko, I.V., D.J. Livingstone, and A.I. Luik, *Neural network studies. 1. Comparison of overfitting and overtraining.* Journal of chemical information and computer sciences, 1995. **35**(5): p. 826-833.
[31] Li, H., et al., *Predicting the higher heating value of syngas pyrolyzed from sewage sludge using an artificial neural network.* Environmental Science and Pollution Research, 2020. **27**(1): p. 785-797.
[32] Liao, M., S.S. Kelley, and Y. Yao, *Artificial neural network based modeling for the prediction of yield and surface area of activated carbon from biomass.* Biofuels, Bioproducts and Biorefining, 2019. **13**(4): p. 1015-1027.
[33] Zhao, S., et al., *Experimental and artificial intelligence study on catalytic reforming of tar over bio-char surface coupled with hydrogen production.* Fuel, 2023. **348**: p. 128563.
[34] Kennedy, J. and R.C. Eberhart. *A discrete binary version of the particle swarm algorithm*. in *1997 IEEE International conference on systems, man, and cybernetics. Computational cybernetics and simulation*. 1997. ieee.
[35] Kennedy, J. and R. Eberhart. *Particle swarm optimization*. in *Proceedings of ICNN'95-international conference on neural networks*. 1995. ieee.
[36] Garro, B.A. and R.A. Vázquez, *Designing artificial neural networks using particle swarm optimization algorithms.* Computational intelligence and neuroscience, 2015. **2015**(1): p. 369298.
[37] Jahed Armaghani, D., et al., *Developing a hybrid PSO–ANN model for estimating the ultimate bearing capacity of rock-socketed piles.* Neural Computing and Applications, 2017. **28**: p. 391-405.

Received: 22.9.2024.
Revised: 23.12.2024.
Accepted: 9.1.2025.

Appendix file

Table 1s. The proximate and ultimate analysis of different solid fuel samples

Material	Proximate analysis/wt%			Ultimate analysis/wt%					HHV
	Ash	VM	FC	C	H	O	N	S	(MJ/kg)
Orange peel	2.44	76.27	21.29	43.93	5.64	48.93	1.34	0.07	18.09
Fruit peel	3.29	77.93	18.78	48.5	6.2	39.5	1.3	0.2	18.63
Rib	38.22	61.56	0.23	51.61	6.38	31.91	9.48	0.62	14.03
Fish bone	39.82	56.25	3.93	63.87	8.01	19.08	8.39	0.64	15.79
Rice	0.4	84.42	15.18	45.97	6.35	45.74	1.69	0.25	18.14
Rice	0.42	87.74	11.84	44.2	5.73	48.75	1.2	0.1	17.97
Rice	1.11	86.45	12.45	43.41	6.29	48.44	1.72	0.13	18.09
China fir	3.53	82.04	14.44	51.47	6.89	41.08	0.4	0.16	20.01
Pine wood	0.95	83.5	15.54	50.51	5.95	43.39	0.11	0.03	19.64
Sawdust	0.42	81	18.58	49.42	7.26	42.92	0.39	0.01	21.17
Wood	3.7	79.45	16.85	50.61	7.45	41.86	0.08	/	18.12
Wood	0.82	81.64	17.54	48.35	6.62	44.7	0.04	0.29	20.69
Wood chips	1.95	82.66	15.4	49.54	6.21	44.06	0.12	0.04	19.16
Wood chips	1.49	87.07	11.45	51.73	4.54	43.5	0.16	0.08	20.18
Wood chips	3.45	81.5	15.05	49.03	5.69	44.98	0.22	0.07	18.59
Wooden chopsticks	2.18	83.5	14.37	48.79	5.16	45.7	0.3	0.04	18.93
Bamboo	1.79	81.36	16.84	51.42	6.01	41.92	0.36	0.29	19.61
Bamboo	0.69	81.03	18.27	50.46	6.32	42.73	0.22	0.1	19.58
Bamboo	1.96	80.56	17.48	50.76	5.91	42.98	0.28	0.07	19.34
Leaves	9.43	74.32	16.25	47.18	5.61	46.35	0.18	0.68	18.36
Leaves	8.92	73.7	17.38	47.25	5.57	46.26	0.19	0.73	17.19
King grass	7.44	74.12	18.43	46.91	5.89	46.3	0.7	0.21	17.98
Blank A4 paper	10.69	79.33	9.98	45.12	5.31	48.91	0.38	0.28	13.51
Magazine	29.49	62.44	8.07	41.04	8.99	49.15	0.42	0.4	11.82
Newspaper	1.38	86.37	12.25	49.1	6.1	43	0.1	0.2	19.73
Newspaper	5.43	85.04	9.53	45.24	7.17	47.1	0.25	0.23	16.27
Newspaper	9.47	78.19	12.33	46.66	6.25	46.86	0.13	0.09	15.34
Printing paper	12.3	87.65	0.04	44.93	4.55	50.43	0.09	0	14.23
Cardboard	9.09	78.8	12.12	49.33	7.94	41.99	0.49	0.25	15.99
Cardboard	5.27	81.75	12.97	46.09	5.36	48.02	0.32	0.21	17.27
Carton	7.22	83.95	8.82	48.97	6.14	44.52	0.21	0.16	17.09
Paper board	14.07	72.27	13.67	49.51	6.29	43.71	0.27	0.22	15.48
Tissue paper	0.04	95.36	4.6	44.31	6.06	49.43	0.13	0.06	16.85
Toilet paper	0.52	90.47	9.01	45.18	6.13	48.32	0.25	0.11	17.25
Cotton	0.41	92.25	7.34	54.2	5.83	39.59	0.29	0.09	21.37
Cotton	0.68	78.27	21.05	49.91	6	43.68	0.26	0.15	17.53
Cotton	0.2	96.2	3.59	44.92	9	45.86	0.19	0.03	15.79
Cotton	1.45	86.7	11.85	46.19	6.12	47.07	0.54	0.08	17.24
Cotton cloth	3.09	78.71	18.21	56.49	5.87	33.3	3.52	0.18	14.21

Cotton cloth	1.52	84.53	13.95	46.51	5.8	46.98	0.43	0.28	17.43
Cotton cloth	0.83	91.65	7.52	45.18	5.66	48.81	0.21	0.14	16.25
Wool	1.24	84.76	14	60.07	4.24	31.48	2.65	1.55	20.92
Acrylic fiber	0.14	75.25	24.61	66.78	5.2	7.31	20.26	0.45	29.77
Polyester taffeta	0.44	90.63	8.93	60.1	4.5	35.11	0.28	0.01	22.08
Terylene	0.49	88.6	10.91	62.16	4.14	33.12	0.29	0.28	20.86
PE	0.06	99.94	0	86.66	13.26	0	0.06	0.02	37.6
PE	0.15	99.85	0	85.94	13.88	0	0.12	0.06	40.98
PE	0.15	99.85	0	85.45	14.32	0	0.16	0.07	46.31
PE	0.3	99.7	0	84.97	14.3	0	0.7	0.02	46.47
PP	0.16	99.84	0	84.3	14.44	1.05	0.18	0.03	45.76
PP	0.02	99.97	0.01	85.41	12.51	1.85	0.23	0	46.23
PET	0.09	90.44	9.47	62.93	4.26	32.64	0.04	0.13	23.09
Rubber	15.28	65.26	19.36	89.18	8.54	0	1.23	1.05	33.4
Rubber	8.36	84.77	6.86	77.72	10.12	7.42	0	2.66	25.17
Rubber	5	74.55	20.44	86.7	7.28	2.14	2.42	1.47	37.29
Tire	3.33	69.25	27.42	85.63	7.86	4.65	0.52	1.34	36.75
Tire	25.7	68.05	6.25	79.19	8.45	11.38	0.69	0.28	26.49
Tire	19.27	63.11	17.61	88.56	8.52	0.88	0.75	1.29	30.16
Tire	4.19	65.44	30.37	83.92	6.83	7.55	0.78	0.92	38.86
Almond shell	2.2	82	15.8	46.35	5.67	47.46	0.3	0.22	18.28
Almond tree branches	5.4	75.6	19	47.35	6.36	45.57	0.65	0.16	18.35
Almond tree leaves	9.3	87.19	3.5	43.25	5.5	48.06	2.85	0.34	17.56
American oak acorn	3.2	74	22.8	44.68	5.98	48.55	0.6	0.18	17.37
Apple tree branches	5	74	21	46.24	11.55	41.01	0.81	0.39	17.82
Apple tree leaves	12	71.9	16.1	44.45	6.15	47.56	1.61	0.23	17.51
Barley grain	3	76.9	20.1	41.59	6.08	50.18	1.79	0.35	16.52
Barley straw	6.1	77.9	16	40.69	6.95	50.5	1.64	0.23	17.37
Bean husk	8	74	18.2	39.66	5.38	53.98	0.66	0.31	15.11
Beetroot pellets	9	76	15	38.94	5.23	54.13	1.19	0.51	15.1
Black polar bark	8	71	20.8	43.25	6.33	49.66	0.42	0.34	17.41
Black poplar leaves	7.8	71.2	21	58.3	8.41	31.92	1.03	0.35	18.17
Black poplar wood	1.5	86	12.3	46.19	5.7	47.36	0.18	0.56	18.39
Briquette	0.8	85	14.2	46.74	6.39	45.52	1.24	0.1	18.5
Building waste chips	0.8	86	13.2	47.26	6.45	46.04	0.08	0.17	18.28
Cherry stone	0.87	85	14.1	48.57	6.21	44.6	0.43	0.19	19.07
Cherry tree branches	4.4	74	21.5	46.42	6.21	46.68	0.52	0.17	19.36
Cherry tree leaves	7.4	71	21.6	45.52	6.25	46.55	1.49	0.19	17.73
Chestnut shell	3.9	67	29.1	42.31	5.17	51.77	0.42	0.33	14.31
Chestnut tree chips	1.3	78.2	20.5	45.3	6.1	48.2	0.23	0.17	17.49
Chestnut tree leaves	4.9	72.41	22.7	47.82	6.24	43.46	2.21	0.27	18.76
Chestnut tree shaving	0.4	79	20.6	45.88	5	48.73	0.12	0.27	17.62
Cocoa beans husk	9.96	69	21	43.25	5.89	47.93	2.64	0.29	17.31
Coconut shell	1.4	79.2	19.4	47.93	6.05	45.63	0.15	0.24	18.88

Coffee husk	5.8	76.2	18	45.06	6.42	45.51	2.53	0.48	18.33
Corncob	2.4	83	14.6	44.78	6.02	48.77	0.22	0.21	17.69
Cypress fruit	4.7	71.8	23.5	27.81	5.7	65.96	0.35	0.18	20.17
Date stone	1.4	82	16.6	43.37	6.23	49.05	1.03	0.32	18.15
Eucalyptus bark	6.2	77	16.8	46.53	5.87	45.61	1.69	0.3	16.24
Eucalyptus chips	1.9	79	19.1	44.77	6.33	48.6	0.14	0.15	16.49
Eucalyptus fruit	4.7	73.6	21.7	46.81	5.81	45.84	1.14	0.39	18.52
Feijoa leaves	6.7	71.2	22.1	45.28	6.03	47.25	1.23	0.2	17.81
Gorse	5	45.2	50.2	43.49	5.53	49.16	1.49	0.33	18.6
Grapevine branches	7.6	71.5	20.9	45	6.95	46.83	0.76	0.46	16.82
Grapevine waste	13.3	73	13.7	35.74	5.95	56.67	1.35	0.3	16.47
Hazelnut and alder chips	5	77	18	45.47	5.94	47.99	0.4	0.2	17.56
Hazelnut shell	2.2	77	20.8	47.8	6.14	45.64	0.27	0.16	18.87
Hazelnut tree leaves	8	79	13.4	45.14	6.79	45.71	2.05	0.31	17.87
Holm oak branch chips	7.4	74.9	17.7	45.65	5.75	45.84	0.76	1.99	17.18
Horse chestnut burr	5.4	70	24.6	53.38	7.16	38.77	0.45	0.23	17.17
Horse chestnut tree br.	6.9	73.5	19.6	43.71	6.27	48.54	1.05	0.43	17.47
Kiwi branches	4.5	74	21.5	46.41	6.09	43.99	1.06	2.44	17.81
Lemon rind	9.7	73.2	17.1	42.95	6.56	48.98	1.08	0.42	17.18
Lemon tree branches	4.7	76.7	18.6	54.74	5.72	38.68	0.54	0.33	17.56
Maize grain	2.1	78.9	19.1	40.96	6.92	50.71	1.17	0.23	16.43
Mimosa branches	4	75	21	45.81	6.19	47.08	0.75	0.17	17.75
Medlar tree braches	8.4	74	17.6	44.36	6.17	48.77	0.52	0.18	17.65
Miscanthus	9.6	79	11.4	47.09	6.3	46.42	0.1	0.1	18.07
Nectarine stone	1.1	76	22.9	48.57	6.22	44.48	0.5	0.23	19.56
Oak acorn	2.6	75.1	22.3	41.84	6.82	50.28	0.8	0.25	16.17
Oak tree branches	4.2	78.4	17.4	48.26	6.28	44.26	2.87	0.33	17.72
Oak tree leaves	3.8	72	24.2	46.9	5.47	44.2	3.04	0.38	18.31
Oak tree pruning	4.3	77	18.7	37.89	5.94	55.23	0.73	0.21	17.59
Oats and vetch	7.33	72	20.7	41.69	5.82	51.27	0.92	0.29	16.66
Oats bran	4.15	77	18.9	44.01	7.17	46.36	2.17	0.29	18.06
Olive stone	1.4	78.3	20.4	46.55	6.33	45.2	1.81	0.11	17.88
Olive tree pruning	13	78	9	45.36	5.47	47.42	1.47	0.28	17.34
Orange tree branches	4.5	79	16.9	45.76	6.12	47.34	0.56	0.21	16.31
Orange tree leaves	15.4	73.2	11.4	41.11	5.28	50.62	2.59	0.4	16.17
Pea husk	4.5	83	12.5	39.62	6.54	50.78	1.24	1.82	15.46
Pea plant waste	5.8	78	15.9	44.06	4.73	49.91	0.9	0.39	17.35
Peach stone	0.5	75.6	23.9	40.72	6.95	48.07	3.94	0.3	19.59
Peach tree leaves	10.2	75	14.7	59.59	9.76	27.86	2.03	0.77	18.34
Peanut shell	2.5	81	16.5	49.35	6.4	42.96	1.05	0.24	20.09
Pepper plant waste	22.9	73.1	4	36.56	5.27	53.67	3.66	0.83	13.66
Pine and eucalyptus chips	3.6	71.6	24.8	45.9	6.3	46.03	1.59	0.19	16.99
Pine chips	0.6	81.6	17.8	48.15	5.59	45.9	0.09	0.28	19.43
Pine kernel shell	2.7	77.6	19.7	47.91	4.9	46.28	0.31	0.6	18.89

Pine pellets	1.3	83.5	15.2	46.83	5.3	47.28	0.28	0.31	18.84
Pine shaving	0.8	85	14.2	48.67	5.08	45.92	0.07	0.26	19.79
Pineapple leaf	3.2	75	21.8	42.26	4.81	52.27	0.4	0.27	18.15
Pinecone heart	3.5	66	30.5	42.22	5.06	51.59	0.29	0.84	16.44
Pinecone leaf	1.3	80	18.7	47.65	5.43	46.21	0.27	0.44	18.63
Pineapple heart	3.5	66	30.5	42.22	5.06	51.59	0.29	0.84	16.44
Pinecone leaf	1.3	80	18.7	47.65	5.43	46.21	0.27	0.44	18.63
Pistachio shell	1.3	82.5	16.2	44.69	5.16	49.87	0.11	0.18	17.35
Plum stone	1.8	77	21.2	48.22	6.6	44.14	0.87	0.17	19.14
Pomegranate peel	6.8	68	25.2	42.19	5.11	51.68	0.69	0.33	15.17
Potato plant waste	15.8	69	14.7	38.33	5.07	55.03	1.13	0.44	15.07
rice husk	13.7	73	13.3	26.69	2.88	70.05	0.21	0.17	15.9
Rye grain	1.8	78.9	19.3	41.11	6.76	50.72	1.2	0.21	16.14
Rye straw	3.2	79.9	16.9	40.18	6.85	51.48	1.16	0.32	17.11
Sainfoin	9.2	73	17.8	41.68	5.9	50.05	1.8	0.57	16.41
Sawdust	1.6	81	17.4	45.34	6.02	47.05	0.53	1.07	18.02
Sorghum	17	62	21	40.79	4.38	53.87	0.73	0.23	11.87
Soya grain	4.8	77	18.2	44.42	6.33	47.86	1.16	0.24	16.71
Straw pellets	9.8	79	11.2	47.89	5.51	45.87	0.56	0.17	16.58
Sunflower seed husk	1.9	80	18.1	45.33	5.91	48.14	0.38	0.24	18
Triticale	6.2	75	18.8	42.14	5.8	50.07	1.23	0.76	16.65
Vegetal coal	5.9	26	68.1	79.34	2.74	16.97	0.65	0.3	29.71
Vine orujillo	12.7	79	8.3	44.15	5.31	48.04	1.91	0.58	17.74
Vine shoot chips	9.7	66	24.3	40.15	5.02	53.91	0.61	0.31	14.63
Vine shoot waste	4.1	64	31.9	34.6	5.61	58.91	0.63	0.24	13.29
Walnut shell	2.3	79	18.7	46.97	6.27	46.44	0.22	0.1	18.38
Wheat bran	3.5	78	18.5	42.74	6.62	47.98	2.34	0.31	17.37
Wheat grain	2.8	80	17.2	49.22	6.52	43.76	0.24	0.26	16.33
Wheat straw	5.3	76	18.2	45.58	6.04	46.6	1.18	0.59	17.34
Wood chips	1.5	68.6	29.9	42.2	5.51	51.88	0.13	0.27	15.16
Wood pellets	1.3	82	17.1	46.7	6.13	46.15	0.6	0.32	18.22
Wood sawdust	0.6	83	16.4	45.97	5.13	48.53	0.12	0.24	18.21
Pistachio soft shell	14.21	67.85	8.69	45.53	5.56	47.17	1.74	/	18.57
Coconut shell	0.71	77.19	22.1	50.22	5.7	43.37	/	/	20.5
Wheat straw	6.9	82.12	10.98	42.95	5.35	46.99	/	/	17.99
Rice husk	21.24	61.81	16.95	38.5	5.2	34.61	0.45	/	14.69
Sugarcane bagasse	3.2	83.66	13.15	45.48	5.96	45.21	0.15	/	18.73
Bamboo wood	1.95	86.8	11.24	48.76	6.32	42.77	0.2	/	20.55
Olive stone	2.2	78.3	19.5	49	6.1	42	0.8	/	20.23
Almond shell	1.1	80.5	18.4	48.8	5.9	43.7	0.5	/	19.92
Esparto plant	2.2	80.5	16.8	46.94	6.44	43.56	0.86	/	19.1
Shea meal	5	66.3	28.7	48.56	5.86	37.3	2.88	/	19.8
Sugarcane bagasse	5.2	81.5	13.3	43.79	5.96	43.36	1.69	/	17.7
Cotton stalk	5,1	76.1	18.8	47.07	4.58	42.1	1.15	/	17.4

Peanut shell	1.7	84.9	13.4	47.4	6.1	44.4	2.1	/	18.6
Hazelnut shell	1.1	68.9	30	50.9	5.9	42.8	0.4	/	19.9
Dried grains	3.89	82.5	12.84	50.24	6.89	33.43	4.79	/	21.75
Corn stover	6.73	66.58	26.65	45.48	5.52	41.52	0.69	/	17.93
Coffee husk	2.4	78.5	19.1	47.5	6.4	43.7	/	/	19.8
Sugar cane straw	9.2	76.2	14.6	43.5	6.1	41.1	/	/	17.19
Soplillo	1.5	77.8	20.7	48.8	6.5	43.2	/	/	22.58
Lantana Camara leaf	7.26	70.46	11.83	45.01	6.68	43.79	2.02	/	18.5
Oil palm fruit bunch	4.53	78.2	16.46	45.9	5.8	40.1	1.2	/	16.96
Olive kernel	1.7	63.9	32.8	54.6	6.8	36.1	0.8	/	22.4
Olive kernel shell	3.3	60.5	36.1	53.2	6.7	36.3	0.5	/	21.4
Olive cake	2.8	62.1	36.1	53.7	6.7	36.2	0.6	/	21.6
Olive kernel	2.13	73.62	24.25	52.44	6.17	37.85	1.32	/	19.9
Forest residue	0.2	79.8	20	53.16	6.25	40	0.3	/	19.5
Cotton residue	6.61	72.8	20.59	47.03	5.96	38.42	1.79	/	16.9
Rice straw	18.67	65.47	15.86	38.24	5.2	36.26	0.87	/	15.09
Switch grass	8.97	76.69	14.34	46.68	5.82	37.38	0.77	/	18.06
Willow wood	1.71	82.22	16.07	49.9	5.9	41.8	0.61	/	19.59
Hybrid poplar	12.49	84.81	2.7	50.18	6.06	40.43	0.6	/	19.02
Almond hulls	6.13	73.8	20.07	47.53	5.97	39.16	1.13	/	18.89
Oak wood	4.05	77.45	18.5	48.76	6.35	42.08	2.81	/	19.2
Pine chips	5.95	72.4	21.65	49.66	5.67	38.07	0.51	/	19.79
Corn straw	7.65	73.15	19.19	44.73	5.87	40.44	0.6	/	17.68
Rape straw	4.65	76.54	17.81	46.17	6.12	42.47	0.46	/	18.34
Palm kernels	5.14	77.28	17.59	48.34	6.2	37.44	2.62	/	20.71
B-wood	1.85	76.53	21.62	50.26	6.91	39.66	1.03	/	20.05
Pepper plant	14.44	64.71	20.86	36.11	4.26	41.86	2.72	/	15.39
Biomass mix	12.49	69.36	18.14	49.59	5.79	28.87	2.43	/	18.4
Sugarcane bagasse	2.7	82.6	14.7	47.2	7	43.1	/	/	17.32
Rice husk	22.5	61.2	16.3	38.2	5.6	33.7	/	/	16.47
Olive pitts	1.72	82	16.28	52.8	6.69	38.25	0.45	/	21.59
Pistachio shell	1.41	81.64	16.95	50.2	6.32	41.15	0.69	/	18.22
Almond shells	3.29	76	20.71	49.3	5.97	40.63	0.76	/	19.49